

# Comment on “Coherence measures for heralded single-photon sources”

Stefano Bettelli

Romanogasse 29/15, 1200 Wien, Österreich

A recent Brief Report [Phys. Rev. A **79**, 035801 (2009)] investigates two figures of merit for heralded photon sources based on spontaneous parametric down-conversion with a continuous pump, namely the time-averaged temporal coherence between the signal and idler beams and the time-averaged *conditioned* second-order degree of coherence for photons in the heralded arm. However, contrary to what is claimed, no one-arm second-order effect is actually measured.

PACS numbers: 42.50.Dv, 03.67.Dd, 42.50.Ar, 42.65.Lm

The phenomenon of spontaneous parametric down-conversion (SPDC) consists in the splitting of a pump photon, in a non-linear crystal, into two modes (arms). A detection in one arm (idler) implies the presence of a photon in the other (signal): the signal photon can thus be heralded in a time window of width  $\tau_d$ , set by the indetermination on the detection time. The probability that a second signal photon shows up in the window is, for sufficiently large windows, essentially  $R\tau_d$ , where  $R$  is the pair-generation rate, which can be made as low as desired. For this reason SPDC-based sources are often used to emulate single-photon sources.

The apparent Poissonian statistics in one arm of the SPDC source[4] observed in the heralded time window is determined by the fact that  $\tau_d$  is often much larger than  $\Delta t$ , the signal coherence time, typically in the range 0.1ps to 1ps; only when  $\tau_d \sim \Delta t$  the thermal nature of SPDC radiation shows up, and the probability of a second photon in the window approaches  $2R\tau_d$ . Experiments on SPDC intrinsic one-arm statistics in single-photon regime are difficult to perform when sources are operated with a continuous pump, since in this case the jitter  $\tau_d$  of single-photon detectors is not better than  $\sim 10^2$ ps. Thermal statistics for one arm of a SPDC source operated in this way was demonstrated only recently [1].

A recent Brief Report by Bocquillon *et al.* [2] (see also the expanded version by Razavi *et al.* [3]), concerning the characterisation of heralded SPDC-based photon sources with a continuous pump, claims “... [to carve] into the theoretical aspects of [measuring] the temporal correlation between the signal and idler beams, and ... the second-order degree of coherence for the heralded signal photons”. More specifically, since the time indetermination of the detection apparatus is orders of magnitude larger than the coherence times of the source, the authors develop a theory connecting the values of the parameters intrinsic to the investigated system to the actually observed averages, and test the theory experimentally. In particular, in the second part of the report, the authors investigate the detection of two photons in the signal arm conditioned on the detection of one photon in the idler arm; clearly this measurement is strictly related to that described in [1], and definitely not less difficult. However, contrary to what is claimed, no one-arm second-order effect is actually measured in [2], as shown in the following.

## Preliminaries

The authors of [2] assume a theoretical model for a low-gain frequency-degenerate type-II SPDC process predicting that all auto- and cross-correlations of the source arms can be expressed by means of the two real even functions  $R(\tau)$  and  $C(\tau)$  shown in Fig.1. In practice  $R(\tau)$  is the first-order coherence of both arms, and  $R(0) = R \sim 43\text{MHz}$  ( $R_{\text{SPDC}}$  in the original text) is the pair-generation rate. With the help of the Gaussian moment-factoring theorem the temporal correlation  $g_{si}^{(2)}(\tau)$  of the signal and the idler, Fig.2, is shown to be sharply peaked for  $|\tau| < \Delta t/2$  (the parameter  $\Delta t \sim 0.3\text{ps}$  plays the role of a signal-idler coherence time):

$$g_{si}^{(2)}(\tau) = \frac{\langle E_s^\dagger(t+\tau)E_i^\dagger(t)E_i(t)E_s(t+\tau) \rangle}{\langle E_s^\dagger(t+\tau)E_s(t+\tau) \rangle \cdot \langle E_i^\dagger(t)E_i(t) \rangle} = 1 + \frac{C^2(\tau)}{R^2(0)} = \begin{cases} 1 + \frac{1}{R\Delta t} & \text{if } |\tau| < \frac{\Delta t}{2} \\ 1 & \text{otherwise} \end{cases} \quad (1)$$

This sharp peak is smeared by detector response times and by the finite coincidence window (implemented in software), respectively characterised by  $\tau_d$  and  $\tau_c$  ( $\tau_{\text{coin}}$  in the original text). The authors of [2] model these effects by means of convolution functions. For the purposes of this Comment it is sufficient to consider  $\tau_c \gg \tau_d$ ; in this case the combined response function of the hardware-software setup is equivalent to a moving-window average with size  $2\tau_c$  and transition regions as large as  $2\tau_d$ . The time-averaged second-order coherence  $\bar{g}_{si}^{(2)}(\tau)$ , pro-

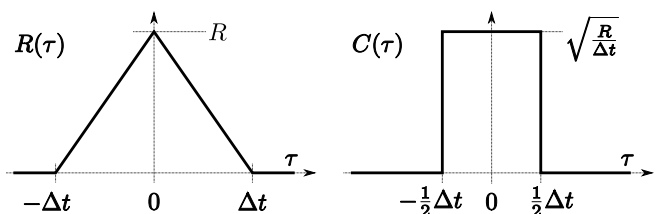


FIG. 1: The signal-signal or idler-idler autocorrelation function  $R(\tau)$ , and the signal-idler cross-correlation function  $C(\tau)$  for the SPDC process analysed in [2].  $R$  is the pair-generation rate, while  $1/\Delta t$  is the bandwidth. Vertical scales are very different since in the actual experiment  $R\Delta t \sim 1.4 \cdot 10^{-5}$ .

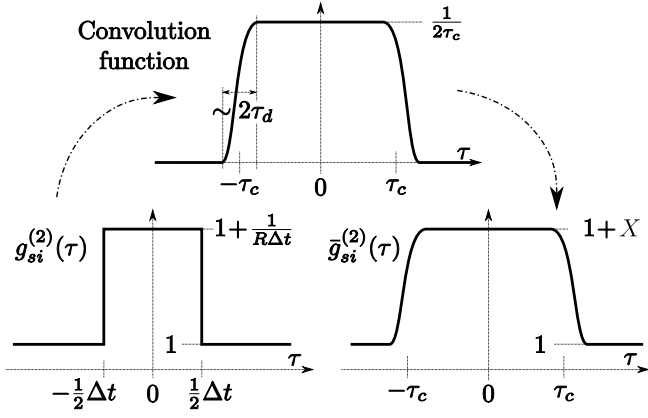


FIG. 2: The second-order coherence function between signal and idler,  $g_{si}^{(2)}(\tau)$ , and its time average,  $\bar{g}_{si}^{(2)}(\tau)$ . The convolution function that transforms the former into the latter is represented on top. Since  $X = (2R\tau_c)^{-1} \sim 10^1$ , the smeared signal-idler correlation peak, though strongly reduced with respect to the ideal one, is still rather simple to measure.

portional to the measured rate of signal-idler coincidences  $N_{si}(\tau)$ , will be equal to one for  $|\tau| > \tau_c + \tau_d$ , and to a constant when  $|\tau| < \tau_c - \tau_d$ , *i.e.*, when the large peak of  $g_{si}^{(2)}(\tau)$  falls in the central part of the convolution window,

$$\bar{g}_{si}^{(2)}(|\tau| < \tau_c - \tau_d) = 1 + \frac{1}{2R\tau_c} \stackrel{\text{def}}{=} 1 + X, \quad (2)$$

where  $X = (2R\tau_c)^{-1}$  is a signal-idler coincidence factor. Since  $R \sim 43\text{MHz}$  and  $2\tau_c < 3\text{ns}$ , the additional term in Eq.2 is still of the order of  $10^1$ , and therefore the signal-idler temporal correlation is relatively easily to demonstrate. Of course, this signal-idler peak could be made arbitrary large by reducing the rate  $R$  (in practice, by reducing the intensity of the pump, as in [3, Fig.4]). At the same time, given that both time scales of the experimental convolution function,  $\tau_d \sim 350\text{ps}$  and  $\tau_c \gtrsim 0.5\text{ns}$ , are several orders of magnitude larger than the coherence time  $\Delta t \sim 0.3\text{ps}$ , the experiment is only sensitive to the integral of the peak, and not to a specific peak model. The behaviour of the average  $\bar{g}_{si}^{(2)}(\tau)$  is illustrated in Fig.2, and agrees with [2, Fig. 2] (also quantitatively, but for the curve at  $2\tau_c = 0.78\text{ns}$  for which  $\tau_d \ll \tau_c$ ).

The authors of the Brief Report claim that good agreement between theory and experimental data proves that their model is particularly accurate, but indeed it is only the dependence on  $\tau_c$  that is truly confirmed, and repeating data analysis with different values is just a test that the software is working correctly.

### Measurement of the conditioned second-order coherence

In the second part of the Brief Report the authors analyse the statistics of signal-signal coincidences con-

ditioned on idler-photon detection, defined as

$$g_c^{(2)}(t_1, t_2 | t_i) = \frac{\langle E_s^\dagger(t_1) E_s^\dagger(t_2) E_s(t_2) E_s(t_1) \rangle_{pm}}{\langle E_s^\dagger(t_1) E_s(t_1) \rangle_{pm} \langle E_s^\dagger(t_2) E_s(t_2) \rangle_{pm}}, \quad (3)$$

where the  $\langle \dots \rangle_{pm}$  averages are performed on post-measurement states (*i.e.*, after detection of an idler photon). By using the operator identity  $\langle Y \rangle_{pm} = \langle E_i^\dagger(t_i) Y E_i(t_i) \rangle \cdot \langle E_i^\dagger(t_i) E_i(t_i) \rangle^{-1}$ , Eq.3 is reduced to

$$g_c^{(2)}(t_1, t_2 | t_i) = \frac{P_{ssi}(t_1, t_2, t_i)}{R^3 \cdot g_{si}^{(2)}(t_1 - t_i) \cdot g_{si}^{(2)}(t_2 - t_i)}, \quad (4)$$

where  $P_{ssi}$  is the ideal triple-coincidence rate that, again with the help of the Gaussian moment-factoring theorem, is proven to be equal to

$$P_{ssi}(t_1, t_2, t_i) = 2C(t_1 - t_i)C(t_2 - t_i)R(t_1 - t_2) + R [R^2 + R^2(t_1 - t_2) + C^2(t_1 - t_i) + C^2(t_2 - t_i)]. \quad (5)$$

Actual measurements are performed with the particular case  $t_1 = t_i$  and  $t_2 = t_i + \tau$  in mind, so that the relevant formula for the numerator of Eq.4 is

$$P_{ssi}(\tau) \stackrel{\text{def}}{=} P_{ssi}(t_i, t_i + \tau, t_i) = 2C(0)C(\tau)R(\tau) + R [R^2 + R^2(\tau) + C^2(0) + C^2(\tau)]. \quad (6)$$

This expression cannot be simplified further, but its behaviour is easy to understand. For delays larger than the coherence time all non-constant terms die out, and  $P_{ssi} \rightarrow R^3 + RC^2(0) = R^3 g_{si}^{(2)}(0)$ ; for  $|\tau| < \Delta t$  the shape is peaked, and its maximum value does not exceed four times its large-delay value, as shown in Fig.3. The denominator of Eq.4, *i.e.*  $R^3 g_{si}^{(2)}(0) g_{si}^{(2)}(\tau)$ , is almost always  $R^3 g_{si}^{(2)}(0)$ , but in the narrow region  $[-\Delta t/2, \Delta t/2]$  it grows several orders of magnitude to reach  $R^3 [g_{si}^{(2)}(0)]^2$ , as can be seen in Fig.2. Therefore the function of interest,  $g_c^{(2)}(\tau) = g_c^{(2)}(t_i, t_i + \tau | t_i)$ , represented in Fig.3, has unit value for  $|\tau| > \Delta t$ , and is  $O(R\Delta t) \sim 10^{-5}$  for  $|\tau| < \Delta t/2$ .

Experimentally measuring a time-averaged version of this well is far from trivial, since the size of the well is only  $O(\Delta t)$ , and the typical convolution spread due to detector jitter and finite coincidence windows is  $\tau_c$ , so

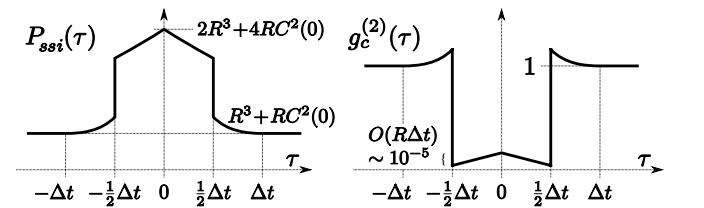


FIG. 3: The triple-coincidence rate  $P_{ssi}(\tau)$ , and the second-order correlation function  $g_c^{(2)}(\tau)$  for an idler photon arriving at time  $t_i$  and two signal photons arriving at  $t_i$  and  $t_i + \tau$ , as defined by [2, Eq.9]. The temporal correlation function is very small ( $\sim 10^{-5}$ ) in the region  $\tau \in [-\Delta t/2, \Delta t/2]$ .

that the effect is in the best case  $O(\Delta t/\tau_d) \sim 10^{-3}$ , and even smaller with the coincidence windows used in the article. This is an effect of the same order of magnitude as that measured in [1] on an almost identical physical system. Instead, Fig.3 of [2] shows a large well extending over 1ns or more. The reason for this strange result is that the authors actually plot the “time-averaged second-order correlation function”  $\bar{g}_c^{(2)}(\tau)$  defined as

$$\bar{g}_c^{(2)}(\tau) = \frac{N_{ssi}(\tau) \cdot R}{N_{si}(0) \cdot N_{si}(\tau)}, \quad (7)$$

where  $N_{si}$  is the already mentioned signal-idler coincidence rate, and  $N_{ssi}$  is the triple signal-signal-idler coincidence rate, proportional to a smeared  $P_{ssi}$ . It is important to understand that even if  $\bar{g}_c^{(2)}$  is studied for  $t_1 = t_i$ , the observable  $N_{ssi}$  is the outcome of a triple-coincidence experiment, and its value is linked to the full three-time structure of  $P_{ssi}$ , shown in Fig.4. Minor details apart,  $P_{ssi}(t_1, t_2, t_i)$  is characterised by three levels: the accidental triple-coincidence plateau at  $R^3$ , the signal-idler coincidence ridges at  $R^3 + RC^2(0)$  (when  $|t_1 - t_i| < \Delta t/2$  or  $|t_2 - t_i| < \Delta t/2$ ), and a more complicated central peak (when both  $t_1, t_2 \in [t_i - \Delta t/2, t_i + \Delta t/2]$ ) where the correlation grows even more, up to a factor four.

The experimental rate  $N_{ssi}$  is obtained by convoluting  $P_{ssi}$  with the response functions of three detectors and two coincidence windows. The effect can be modelled as a moving average with a square bidimensional averaging window of area  $(2\tau_c)^2$  and transition regions of size  $2\tau_d$ . The value of  $N_{ssi}$  will then be significantly different from  $R^3$  only when the averaging window is close to one of the ridges of Fig.4; due to translation invariance the result is  $R^3[1 + X]$  as before. But when the averaging window sits at  $t_1 = t_2 = t_i$  both ridges participate to the average and their contribution is twice as large:  $R^3[1 + 2X]$ . Note that the complicated peak at the ridge junction is almost irrelevant since its contribution relative to  $R^3 X$  is only  $O(\Delta t/\tau_c) \sim 10^{-3}$ , due to its height being limited and its base being only  $\Delta t \times \Delta t$ , and not  $\Delta t \times \tau_c$  as for the part of each ridge within the averaging window.

The conclusion of the previous discussion is that the expected shape of the coincidence functions [5] are

$$N_{ssi}(\tau) \sim \begin{cases} R^3(1 + 2X) & \text{for short delays,} \\ R^3(1 + X) & \text{for long delays,} \end{cases} \quad (8)$$

$$\text{and } N_{si}(\tau) = \begin{cases} R^2(1 + X) & \text{for short delays,} \\ R^2 & \text{for long delays,} \end{cases} \quad (9)$$

where “long” and “short” delays mean approximately  $|\tau| > \tau_c + \tau_d$  and  $|\tau| < \tau_c - \tau_d$  respectively. It is not surprising that only the accidental-coincidence factor,  $R^3$ , and the signal-idler coincidence-peak factor,  $X = (2R\tau_c)^{-1}$ , show up in the formula for  $N_{ssi}$ : all signal-signal effects are in fact too small to be detectable unless explicitly looked for. The graph of  $\bar{g}_c^{(2)}(\tau)$ , Eq.7,

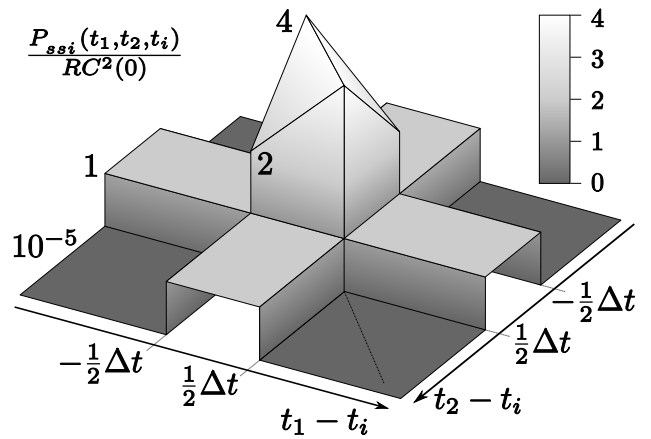


FIG. 4: The ideal triple-coincidence rate  $P_{ssi}(t_1, t_2, t_i)$  (only most relevant structures shown). The ridges running parallel to the axes  $t_1 = t_i$  and  $t_2 = t_i$  are given by signal-idler correlation. When both  $t_1$  and  $t_2$  are very close to  $t_i$  correlations are increased by a factor at most four.  $P_{ssi}$  is symmetric under  $t_1 \leftrightarrow t_2$ , i.e., around the dash-dotted bisector. The function floor is the accidental triple rate  $R^3$ .

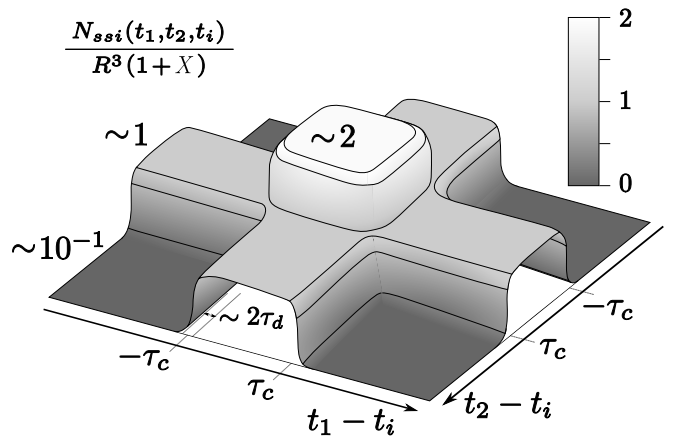


FIG. 5: The expected experimental triple-coincidence rate  $N_{ssi}(t_1, t_2, t_i)$ , obtained from the ideal triple-coincidence rate  $P_{ssi}(t_1, t_2, t_i)$  of Fig.4 by means of a moving bidimensional averaging window of area  $4\tau_c^2$  and transition regions of size  $2\tau_d$ . The central structure is in practice not related to the central peak of Fig.4. The scales of time axes in Fig.4 and 5 differ by more than three orders of magnitude. The floor of the function is again the accidental triple rate  $R^3$ .

is therefore

$$\bar{g}_c^{(2)}(\tau) = \begin{cases} \sim \frac{1+2X}{(1+X)^2} \sim 4R\tau_c & \text{for short delays} \\ 1 & \text{for long delays.} \end{cases} \quad (10)$$

This conclusion is quantitatively confirmed by visual inspection of [2, Fig. 3 and Fig. 4] (in the limit  $\tau_c \gg \tau_d$  of course[6]). Therefore, far from addressing the probability of detecting two signal photons conditioned on the detection of an idler photons, these authors are again just measuring the temporal correlation between the signal and idler arm.

### Meaning of the conditioned second-order coherence

Let us come back to the definition of second-order signal coherence *conditioned* on the detection of an idler photon at time  $t_i$ , given in Eq.3. This is the standard definition of Glauber's  $g^{(2)}$ , but over a post-measurement state obtained by applying the idler measurement operator to the unconditioned SPDC density matrix:

$$\rho \longrightarrow \rho_{t_i} = \frac{E_i(t_i) \rho E_i^\dagger(t_i)}{\text{tr}[\rho E_i^\dagger(t_i) E_i(t_i)]}. \quad (11)$$

The resulting state is of course not time invariant, because of the introduction of the parameter  $t_i$ . Equivalently, one can use modified observables for the evaluation of expectation values on the original state:

$$\langle Y \rangle_{\text{pm}} \longrightarrow \frac{\langle E_i^\dagger(t_i) Y E_i(t_i) \rangle}{\langle E_i^\dagger(t_i) E_i(t_i) \rangle}. \quad (12)$$

The usefulness of the  $g^{(2)}(t_1, t_2)$  function for a *time-invariant* field is that it is insensitive to detector efficiencies and depends only on  $\tau = t_2 - t_1$ , proportional to the probability (or rate, for a continuous field) of finding two photons at times  $t_1$  and  $t_2$ . If  $g^{(2)}(\tau)$  decreases (increases) in some neighbourhood of  $\tau = 0$  the field is said to be *bunched* (*anti-bunched*), meaning that photons “prefer” to come together (alone). If  $g^{(2)}(0)$  is smaller (larger) than one the field statistics in a sufficiently small time window is sub-Poissonian (super-Poissonian).

However, due to the introduction of the idler time  $t_i$ , the conditioned SPDC field is no more time invariant, and  $g_c^{(2)}$  turns out not to be proportional to the rate of arrival of signal photons at time  $t_1$  and  $t_2$ , because the normalisation factors in the denominator of Eq.3 are not constant. For instance, if  $t_2$  is set to a very large time, using Eqs.4, 5, and 1 it is immediate to find that

$$g_c^{(2)}(t_1, t_2 = \infty | t_i) = 1, \quad (13)$$

irrespectively of the delay  $t_1 - t_i$ , although the detection rate on the first signal detector is much larger when

$t_1 = t_i$  with respect to the case  $t_1 - t_i \gg \Delta t$ , due to signal-idler correlation. Therefore  $g_c^{(2)}$  is not a good substitute for detection rates; one should instead directly use the probability density of detecting signal photons at times  $t_1$  and  $t_2$  provided an idler photon was detected at time  $t_i$ , which, due to Bayes' theorem, is just the triple-coincidence rate  $P_{ssi}(t_1, t_2, t_i)$  divided by  $R$ .

It is also to be remarked that the last two special cases described in [2, pag.3, right], which should presumably corroborate the idea that  $g_c^{(2)}$  is a sensible figure of merit, can also be obtained from  $P_{ssi}$ . Specifically, these examples concern the fact that  $\Delta t$  is the signal-idler “coherence time”,

$$\frac{P_{ssi}(t_1, \infty | t_i)}{P_{ssi}(-\infty, \infty | t_i)} = 1 + \frac{C^2(t_1 - t_i)}{R^2} = g_{si}^{(2)}(t_1 - t_i),$$

and that unconditioned signal-signal events are thermal,

$$\frac{P_{ssi}(t_1, t_2 | -\infty)}{P_{ssi}(t_1, \infty | -\infty)} = 1 + \frac{R^2(t_1 - t_2)}{R^2} = 1 + |g_s^{(1)}(t_1 - t_2)|^2.$$

On the other hand, instead of showing any sign of sub-Poissonian behaviour, as the last special case  $g_c^{(2)}(t_i, t_i | t_i) \sim 0$  seems to suggest, the point  $t_1 = t_2 = t_i$  is the maximum of  $P_{ssi}$ . This is in agreement with the fact that one-arm SPDC radiation is thermal: if an idler photon was detected at time  $t_i$  and a signal photon at time  $t_1 = t_i$ , then the most likely time for a second signal photon to appear is just  $t_2 = t_i$ .

### Conclusions

It is shown that the experimental findings reported in [2, Fig. 3 and 4] about conditioned signal-signal coincidences in an SPDC source are indeed related not to the conditioned second-order signal-signal coherence, but to the much simpler (to measure) and stronger signal-idler correlation. The author acknowledges fruitful discussions on the subject with H. Hübel and I. M. Herbauts.

- 
- [1] B. Blauensteiner, I. Herbauts, S. Bettelli, A. Poppe, and H. Hübel, *Photon bunching in parametric down-conversion with continuous wave excitation*, Phys. Rev. A **79**, 063846.
- [2] E. Bocquillon, C. Couteau, M. Razavi, R. Laflamme, and G. Weihs, *Coherence measures for heralded single-photon sources*, Phys. Rev. A **79**, 035801 (2009).
- [3] M. Razavi, I. Söllner, E. Bocquillon, C. Couteau, R. Laflamme, and G. Weihs, *Characterizing heralded single-photon sources with imperfect measurement devices*, J. Phys. B: At. Mol. Opt. Phys. **42**, 114013 (2009).
- [4] The statistical properties described in this paragraph are discussed at length in the introduction of Ref. [1].
- [5] A plot of  $N_{ssi}$  is not available in Ref.[2], but it is given in [3, Fig. 5], and it corresponds to the analysis just given

(see Fig.5 here). The authors of [3] claim that the peak at the centre of [3, Fig. 5] represents the contribution of multiple photon pairs, but this is clearly wrong, since it is just an artifact of the averaging method. In fact, the peak height is twice as large as the height along the ridges, and not more as should be expected from Fig.4 (the authors blame this discrepancy on the 50/50 beam-splitter, but this explanation is incorrect since the beam-splitter influences all rates in the same way).

- [6] If  $\tau_c \gg \tau_d$  but the convolution time scale is still much larger than  $\Delta t$ , then Eqs.8-10 hold valid with  $X = p/R$ , where  $p$  is the height of the plateau of the convolution function.